

Expression Are Induced by Hepatitis C Virus Core Protein

MICHIARI OKUDA,^{*,†} KUI LI,[†] MICHAEL R. BEARD,[†] LORI A. SHOWALTER,^{*} FRANK SCHOLLE,[†] STANLEY M. LEMON,^{†,§} and STEVEN A. WEINMAN^{*,§}

Departments of ^{*}Physiology and Biophysics, [†]Microbiology and Immunology, and [§]Internal Medicine, University of Texas Medical Branch, Galveston, Texas

See editorial on page 568.

Background & Aims: The mechanisms of liver injury in chronic hepatitis C virus (HCV) infection are poorly understood. Indirect evidence suggests that oxidative stress and mitochondrial injury play a role. The aim of this study was to determine if the HCV core protein itself alters mitochondrial function and contributes to oxidative stress. **Methods:** HCV core protein was expressed in 3 different cell lines, and reactive oxygen species (ROS) and lipid peroxidation products were measured. **Results:** Core expression uniformly increased ROS. In 2 inducible expression systems, core protein also increased lipid peroxidation products and induced antioxidant gene expression as well. A mitochondrial electron transport inhibitor prevented the core-induced increase in ROS. A fraction of the expressed core protein localized to the mitochondria and was associated with redistribution of cytochrome c from mitochondrial to cytosolic fractions. Sensitivity to oxidative stress was also seen in HCV transgenic mice in which increased intrahepatic lipid peroxidation products occurred in response to carbon tetrachloride. **Conclusions:** Oxidative injury occurs as a direct result of HCV core protein expression both in vitro and in vivo and may involve a direct effect of core protein on mitochondria. These results provide new insight into the pathogenesis of hepatitis C and provide an experimental rationale for investigation of antioxidant therapy.

Infection with hepatitis C virus (HCV) is a leading cause of chronic hepatitis, and current therapy results in viral elimination in fewer than 50% of individuals.¹ The mechanisms underlying HCV-associated liver cell injury are not well understood; in particular, the relative contributions of immune and direct viral effects are not known. Oxidative stress, imposed either directly by the virus or by the host-immune response, has been suggested as a potentially important pathologic mechanism in hepatitis C as well as other chronic liver diseases.²

Liver tissue from HCV-infected patients shows evidence of glutathione depletion, morphologic changes in mitochondria,³ and the presence of lipid peroxide-protein adducts.⁴ Plasma samples also show increased lipid peroxidation products,⁵ and peripheral blood mononuclear cells from hepatitis C virus (HCV)-infected patients contain elevated superoxide dismutase activity,⁶ consistent with a response to increased cellular reactive oxygen species (ROS). A link between oxidative stress and pathogenesis is also supported by a pilot study of antioxidant therapy that suggested improvements in liver injury in chronic hepatitis C.⁷

Despite this evidence, little is understood about the mechanisms that produce oxidative stress in chronic hepatitis C. We show that HCV core protein alters mitochondrial function and results directly in an increase in the cellular abundance of ROS with consequent increases in cellular lipid peroxidation. These results provide new insight into how HCV infection leads to hepatic injury, and provide a firm theoretical basis for the investigation of antioxidant therapies in this important disease.

Materials and Methods

Cell Lines

Human hepatoma Huh-7 cells were maintained in Dulbecco modified Eagle medium supplemented with 10% heat-inactivated fetal bovine serum, penicillin G (100 U/mL), streptomycin (100 U/mL; Gibco-BRL, Rockville, MD) in a humidified 37°C/5% CO₂ incubator. HeLa Tet-Off cells (Clontech, Palo Alto, CA) were cultured in the same medium except for the addition of 100 µg/mL G418. The complementary DNA (cDNA) fragment encoding full-length HCV core

Abbreviations used in this paper: CM-DCF, chloromethyl 2',7'-dichlorodihydrofluorescein diacetate; DPI, diphenyliodonium; ER, endoplasmic reticulum; MPT, mitochondrial permeability transition; ROS, reactive oxygen species.

© 2002 by the American Gastroenterological Association

0016-5085/02/\$35.00

doi:10.1053/gast.2002.30983

protein of an infectious cDNA clone (genotype 1b)⁸ was inserted into pTRE2 (Clontech) to generate pTRE2-191. Cells were cotransfected with pTet-Off (Clontech) and pTRE2-191 (Huh-7) or pTRE2-191 and pTK-Hyg (Clontech; HeLa), followed by selection with 400 $\mu\text{g}/\text{mL}$ G418 (Huh-7) or 200 $\mu\text{g}/\text{mL}$ hygromycin (HeLa) and 1 $\mu\text{g}/\text{mL}$ tetracycline (Sigma-Aldrich, St. Louis, MO). G418-resistant Huh-7 clones and G418/hygromycin double-resistant HeLa clones were examined for core protein expression upon withdrawal of tetracycline by immunofluorescence microscopy and immunoblot analysis. A Huh-7 clone (191-20) and a HeLa clone (191-14) with tight conditional expression of core were selected for further study.

Measurement of Cellular DNA Content

Huh-7 191-20 cells were seeded in T-175 flasks at a density of 5×10^5 cells and grown to 80% confluence for 5 days in the presence or absence of tetracycline. Cells were trypsinized, and cell cycle distribution was determined by propidium iodide staining for DNA content followed by flow cytometry as described previously.⁹ Briefly, 2.5×10^6 cells were pelleted and washed with cold phosphate-buffered saline (PBS)/azide solution (PBS plus 0.1% sodium azide). Cells were resuspended in 1 mL of low-salt staining buffer (3% PEG 8000 [wt/vol], 50 $\mu\text{g}/\text{mL}$ propidium iodide, 180 U/mL RNase A, 0.1% (vol/vol) Triton X-100, 4 mmol/L sodium citrate) and incubated at 37°C for 20 minutes. One milliliter of high-salt staining buffer (3% PEG 8000 [wt/vol], 50 $\mu\text{g}/\text{mL}$ propidium iodide, 180 U/mL RNase A, 0.1% [vol/vol] Triton X-100, 400 mmol/L sodium chloride) was added to the cells followed by incubation at 4°C overnight. Stained nuclei were analyzed by flow cytometry on a Becton-Dickinson (San Jose, CA) FACScan flow cytometer. Percentages of cells in various stages of the cell cycle were determined using the WinMDI 2.8 flow cytometry software package.

Measurement of ROS

Cells were plated onto glass coverslips and examined for ROS production 72 hours after removal of tetracycline. They were loaded for 2 hours with chloromethyl 2',7'-dichlorodihydrofluorescein diacetate (CM-DCF; Molecular Probes, Inc., Eugene, OR) at a final concentration of 10 $\mu\text{mol}/\text{L}$. Fluorescence was measured by quantitative single-cell fluorescence microscopy at 495 nm/535 nm (excitation/emission) using an Image-1/FL analysis system as described previously.¹⁰ Results were expressed as relative fluorescence intensity and normalized to control cells. In some experiments, ROS was measured after addition of diphenyliodonium (100 $\mu\text{mol}/\text{L}$; Aldrich, Milwaukee, WI) or cyclosporin A (5 $\mu\text{mol}/\text{L}$; Sigma).

Measurement of LPO Products

Appropriate cell cultures ($2\text{--}4 \times 10^7$ cells) or tissue homogenates (200 mg liver tissue) were prepared by sonication and stored at -70°C with 5 mmol/L butylated-hydroxytoluene (Sigma). For cells expressing core protein, samples were obtained 72 hours after removal of tetracycline. 4-Hy-

droxyalkenals and malondialdehyde were measured in these homogenates using a commercial assay (LPO-586; OXIS International Inc., Portland, OR). Protein concentration was determined by the Coomassie assay (Pierce, Rockford, IL).

Carbon Tetrachloride Treatment of Transgenic Mice

Transgenic mice (S-N/863 lineage) were used. These mice are a heterozygous model and express the HCV structural proteins (core, E1, and E2p7) in hepatocytes under the control of the murine albumin enhancer/promoter. Their characteristics are described in detail in this issue of *GASTROENTEROLOGY* (Lerat et al. 2002;122:352–365). Transgenic mice and their normal C57BL/6 littermates were injected intraperitoneally with 20 $\mu\text{L}/\text{kg}$ of CCl_4 (Aldrich, Milwaukee, WI) in olive oil. Control mice were injected with an equal volume of olive oil. Animals were killed 24 hours after CCl_4 injection, and liver tissue and blood samples were collected for determination of histology, lipid peroxidation products, and alanine aminotransferase. All procedures were approved by and carried out in accordance with the policies of the Institutional Animal Care and Use Committee of the University of Texas Medical Branch.

Fluorescence Microscopy

Cells were grown on plastic culture slides and incubated at 37°C for 30 minutes with MitoTracker Red (50 nmol/L; Molecular Probes, Inc.). Cells were fixed in 3.7% paraformaldehyde and permeabilized with 0.25% saponin in PBS. Fixed cells were subsequently incubated with mouse monoclonal anti-hepatitis C core antibody (Affinity Bioreagents, Golden, CO) at a dilution of 1:350 for 2 hours at room temperature and with Alexa Fluor 488 goat anti-mouse IgG (Molecular Probes, Inc.) at a dilution of 1:500 for 30 minutes at 37°C and incubated with DAPI (1 $\mu\text{mol}/\text{L}$; Sigma) for 4 minutes. They were examined with a Nikon Eclipse epifluorescence microscope or a Zeiss LSM-410 confocal microscope. Mitochondrial permeability transition (MPT) was assessed by a modification of the method described by Nieminen et al.¹¹ Cells were loaded by exposure to rhodamine-123 (Molecular Probes, Inc.) for 0.5–2 hours, perfused with Na-Ringers solution, pH 7.7, 37°C, and serially imaged with epifluorescence microscopy at 12-min intervals. The onset of MPT was determined by the sudden loss of fluorescence from mitochondria.

Subcellular Fraction and Immunoblotting

Cells were suspended in HIM buffer¹² supplemented with 10 $\mu\text{L}/\text{mL}$ of protease inhibitor cocktail (Sigma), homogenized with a tight-fitting Dounce homogenizer (25 strokes) and centrifuged at 10,000g for 10 minutes to collect the crude mitochondria. Purified mitochondria were prepared by Percoll gradient centrifugation as described.¹³ The postmitochondrial supernatant was centrifuged at 100,000g for 30 minutes to obtain a cytosolic fraction.

For immunoblotting, samples were separated by sodium dodecyl sulfate–polyacrylamide gel electrophoresis on a 16%

gel and electrophoretically blotted onto polyvinylidene difluoride membranes (BioRad). Protein quantities applied were 50 μ g of whole-cell lysate for detection of core; 2.5 μ g of crude mitochondrial and 17 μ g of cytosolic fraction for detection of cytochrome c; and 7 μ g of both crude and pure mitochondrial fractions for detection of core, coxII, and calnexin. Proteins were detected with the enhanced chemiluminescence plus Western blotting detection system (Amersham, Little Chalfont, Buckinghamshire, England). Primary antibodies used were mouse monoclonal anti-HCV core (Maine Biotechnology Services, Inc., Portland, ME) at 1:25 dilution, mouse monoclonal anti-cytochrome c antibody (R & D Systems, Inc., Minneapolis, MN) at 1:2000 dilution, mouse monoclonal anti-human cytochrome oxidase subunit II antibody (Molecular Probes) at 1:500 dilution, and mouse monoclonal anti-calnexin antibody (Affinity Bioreagents) at 1:500 dilution.

RNA Isolation and Analysis With High-Density Oligonucleotide Arrays

High-density oligonucleotide arrays were probed with biotinylated single-stranded antisense RNAs prepared from total cellular RNA isolated from Huh-7 and Huh-7/191-20 cells before and after induction of HCV core protein expression. RNA was extracted using the RNeasy RNA extraction kit (Qiagen, Crawfordsville, IN) and used as a template for probe synthesis in a reaction according to the manufacturer's protocol (Affymetrix, Santa Clara, CA). Biotinylated probes were then hybridized to an Affymetrix human GeneChip (Hu95A). The DNA arrays were scanned using an Affymetrix confocal scanner (Agilent), and the data were analyzed using Microarray GeneSuite software 4.0.1. Only mRNAs that showed a ≥ 3 -fold differential regulation between cells expressing HCV core protein and those not expressing core protein were selected for further analysis.

Statistical Analysis

Statistical analyses were carried out by unpaired or paired *t* test as appropriate. All data are reported as means \pm SD or SE. A *P* value of <0.05 was considered significant.

Results

Core Protein Expression in Inducible Cell Lines

We developed clonal, stably transformed cell lines from human hepatoma (Huh-7/191-20) and human cervical carcinoma cells (HeLa/191-14) capable of conditionally expressing the full-length HCV core protein (amino acids 1–191) under control of the Tet-Off promoter. Figure 1A shows the tight control of core protein expression in both Huh-7/191-20 and HeLa/191-14 cells. In both cell lines there was no detectable core protein when cells were cultured in the presence of tetracycline, but strong core protein expression was detected 72 hours after the withdrawal of tetracycline from

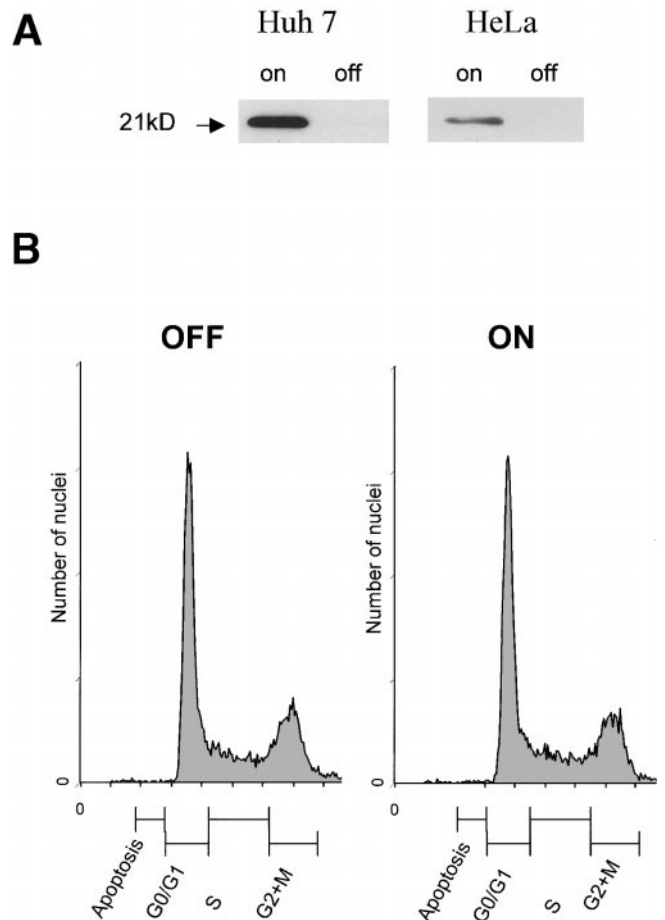


Figure 1. HCV core protein expression and cellular DNA content. (A) Huh-7/191-20 and HeLa/191-14 cells were cultured in the presence (off) or absence (on) of tetracycline, and immunoblotting for HCV core protein was performed on whole-cell lysate as described. The expected molecular weight for core protein (21 kilodaltons) is indicated. (B) Cellular DNA content was measured by flow cytometry in Huh-7/191-20 cells. There was no difference in the distribution of cells through the cell cycle as a result of core protein expression.

the culture medium. Maximal core protein expression in Huh-7/191-20 cells was estimated by comparison of Western blots with known quantities of synthetic core protein (kindly provided by S. Watowich) and was approximately 60 ng core/mg cell protein.

To determine if core protein expression alters apoptosis or cell growth, we subjected cells to flow cytometric measurement of DNA content. The results, shown in Figure 1B, show no difference in the distribution of cells through the cell cycle as a result of core protein expression. In particular, there was no change in the small population of subdiploid cells, indicating that the incidence of spontaneous apoptosis is small and not affected by core protein expression. Furthermore, induction of core protein did not alter cell growth rates as assessed by cell counts in dividing cultures (Li et al., manuscript in preparation).

Core Protein Expression Increases Cellular ROS

The ROS content of Huh-7/191-20 cells and HeLa/191-14 cells was determined by a single-cell fluorescence assay before (off) and after (on) the induction of core protein expression. As shown in Figure 2A, the

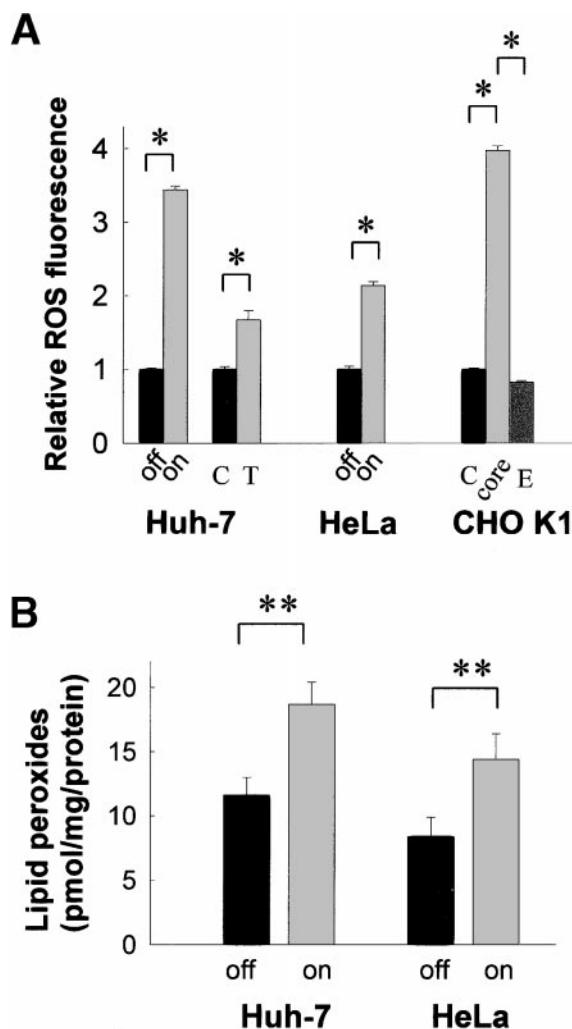


Figure 2. HCV core protein expression increases cellular ROS levels. (A) ROS was measured as single-cell fluorescence after exposure of cells to CM-DCF for 2 hours. Results are expressed as relative brightness and normalized to control cells. Huh-7/191-20 cells were incubated for 72 hours with (off, $n = 1114$) or without (on, $n = 1140$) tetracycline. Parental Huh-7 cells were cultured under control conditions (C, $n = 180$) or for 2 hours in the presence of tumor necrosis factor α (30 ng/mL) and actinomycin D (0.5 $\mu\text{g}/\text{mL}$; T; $n = 32$). Core protein-inducible HeLa/191-14 cells (off, $n = 514$; on, $n = 514$) and stably transfected CHO-K1 cells expressing core/E1/E2 proteins (core, $n = 2861$) or E1/E2 proteins (E, $n = 2950$) were also used as indicated. (B) Total cellular lipid peroxidation products, 4-hydroxyalkenals (4-HNE) and malondialdehyde (MDA), were determined by colorimetric lipid peroxidation assay (LPO-586) from cellular extracts. Induction of core protein expression resulted in a 2-fold elevation in lipid peroxide products in both Huh-7 and HeLa cells ($P < 0.05$). The experiment was repeated 4 times in Huh-7 cells and 8 times in HeLa cells.

expression of core increased the basal ROS content of Huh-7/191-20 cells 3.4 ± 0.05 -fold ($P < 0.001$). As a control, we also measured ROS in normal Huh-7 cells after treatment with tumor necrosis factor α (100 ng/mL; Endogen, Rockford, IL) and actinomycin D (0.5 $\mu\text{g}/\text{mL}$; Sigma), a proapoptotic stimulus that has previously been shown to produce apoptosis and oxidative stress in hepatocytes.¹⁴ This treatment produced a 1.7-fold increase in ROS content compared with control Huh-7 cells ($P < 0.001$), less than that resulting from expression of core protein. ROS abundance was also increased in HeLa/191-14 cells upon induction of core protein expression and in stably transformed Chinese hamster ovary (CHO-K1) cells expressing core, E1, and E2p7 ($P < 0.001$) but not in CHO-K1 cells expressing E1 and E2p7 only¹⁵ (Figure 2A). Together, these results provide strong evidence that ROS accumulation is caused specifically by expression of the core protein.

We next quantified total cellular lipid peroxidation products in extracts from these cells. This information provides a measure of the consequences of oxidative stress because peroxidation of lipids is a result of elevated cellular ROS. The induction of core protein expression resulted in a significant increase in the abundance of lipid peroxide products in both Huh-7/191-20 and HeLa/191-14 cells (Figure 2B). This result confirms that core protein expression induces oxidative injury in these cells.

Role of Mitochondria in Core-Induced ROS Production

ROS are generated as a consequence of mitochondrial electron transport caused by a small proportion of the electron flow interacting with molecular oxygen before reaching the cytochrome oxidase complex.¹⁶ Mitochondria are the principal source of cellular ROS under most conditions, and the mitochondrial component of ROS production can be quantitatively inhibited by diphenyliodonium (DPI), an irreversible inhibitor of flavoenzymes that blocks electron transport through mitochondrial complex I¹⁷ and thus prevents mitochondrial ROS production.¹⁸ Figure 3A shows that DPI treatment (100 $\mu\text{mol}/\text{L}$) entirely inhibited the increase in cellular ROS level that followed the induction of core protein. Under these conditions there was no effect of DPI on cell death as assessed by trypan blue exclusion or morphology. This result is consistent with mitochondria being the source of the increase in ROS. Rotenone and antimycin A, 2 other mitochondrial respiratory chain inhibitors, were also evaluated, but as previously noted,¹⁹ both of these inhibitors greatly increased ROS production in control cells and thus were not useful for determining the source of core-induced ROS.

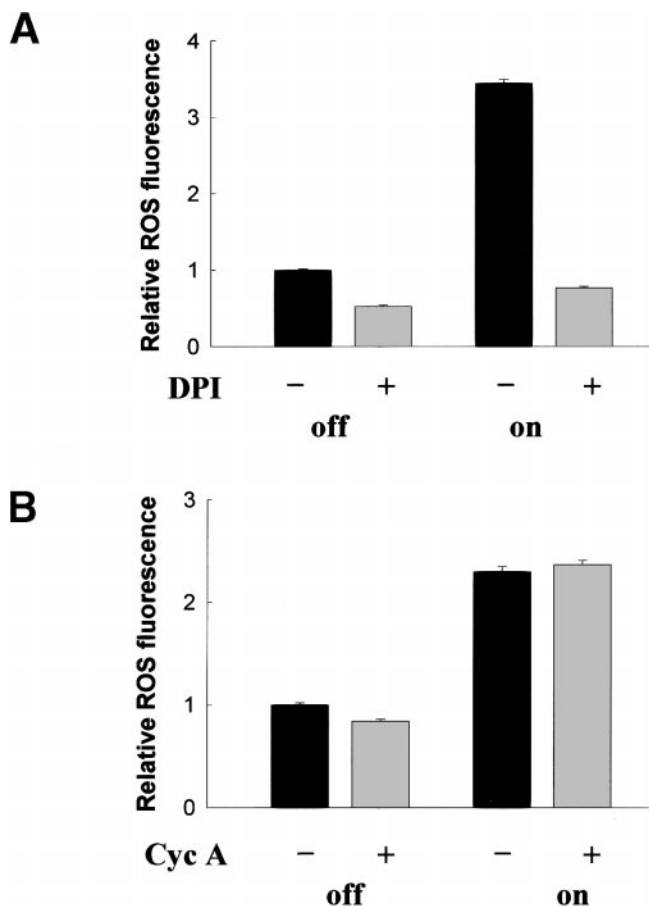


Figure 3. Mitochondria are the source of core-induced ROS. (A) DPI (100 $\mu\text{mol/L}$) was added to the HCV core protein-expressing ($n = 637$) and -nonexpressing ($n = 600$) Huh-7 cells for 3 hours. (B) Cyclosporin A (Cyc A, 5 $\mu\text{mol/L}$) was added to the on ($n = 355$) and off ($n = 370$) cells for 20 hours before measurement of ROS content.

We next examined whether the MPT plays a role in core protein-induced accumulation of ROS. Cells were loaded with a fluorescent organic cation, rhodamine-123, which is accumulated in mitochondria as a result of the negative intramitochondrial potential. The onset of MPT was determined by the sudden loss of rhodamine-123 fluorescence from mitochondria. Spontaneous MPT did not occur within 8 hours of observation, and core protein expression by itself did not induce MPT by this assay. MPT was next induced by continuous exposure of cells to *t*-butylhydroperoxide (tBOOH, 25 $\mu\text{mol/L}$). In control cells, MPT occurred after a period of 2.1 ± 0.2 hours ($n = 38$). Expression of core protein had no effect on the sensitivity or time required for tBOOH-induced MPT. Permeability transition was significantly delayed by the presence of the MPT inhibitor cyclosporin A (2.9 ± 0.3 hours, $n = 32$; $P < 0.001$). Despite its ability to delay MPT, cyclosporin A had no effect on the core-induced increase in ROS abundance (Figure 3B). This suggests

that MPT does not play a role in the accumulation of ROS associated with core protein expression.

Association of Core Protein With Mitochondria

Because these results suggest the possibility of a direct effect of core protein on mitochondrial function, the spatial relationship between core protein and mitochondria was determined by fluorescence microscopy. Figure 4 shows the relationship between indirect immunofluorescence for core protein (green) and mitochondria (stained with MitoTracker Red). Epifluorescence images (Figure 4A–C) show that core protein is expressed in a vesicular pattern that is largely distinct from the more filamentous mitochondria. However, there were numerous areas of overlap between mitochondria and the core protein, particularly in the perinuclear region. We fur-

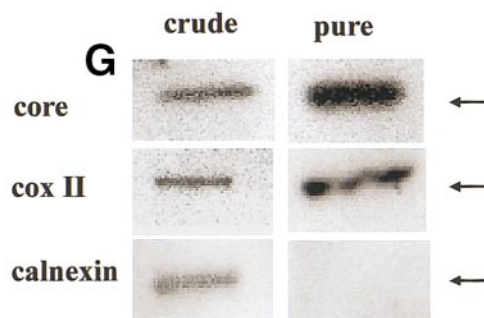
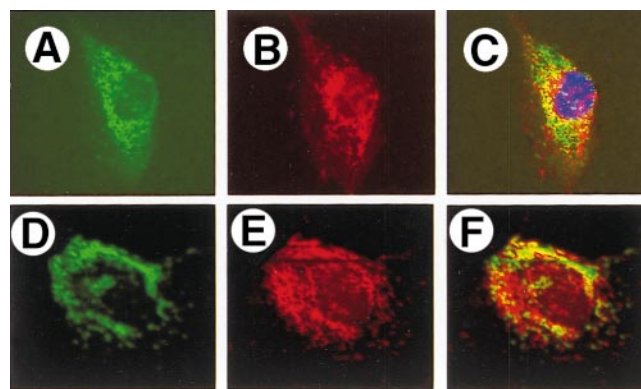


Figure 4. Intracellular distribution of HCV-core protein. Huh-7/191-20 cells were grown in the absence of tetracycline, stained with MitoTracker Red for mitochondria, DAPI (blue) for nuclei, and indirect immunofluorescence (green) for core protein and examined by (A, B, C) epifluorescence or (D, E, F) confocal microscopy. Images of (A, D) core protein and (B, E) mitochondria are shown. In the composite of both images (C, F), areas of colocalization appear as a yellow color. The depth of field for the confocal images is 1.0–1.5 μm . (G) Immunoblotting for HCV core protein, an intrinsic mitochondrial protein (cytochrome oxidase, cox II), and an ER protein (calnexin) were performed in crude and pure mitochondrial fractions as described. The expected molecular weights are indicated.

ther examined the possibility of colocalization using confocal microscopy producing images with a depth of field of 1.5 μm (Figure 4D, E). These images show colocalization of core and mitochondria in several locations, particularly in the perinuclear location.

To further evaluate the possibility that core protein associates with mitochondria, we determined the distribution of core among subcellular fractions. In Huh-7/191-20 cells, most of the core protein was present in a crude mitochondrial fraction (Figure 4G), whereas no core protein was detectable in the cytosol (data not shown). However, immunoblot analysis of the crude mitochondrial fraction with antibodies specific for calnexin (an endoplasmic reticulum [ER] protein) and cytochrome oxidase (an intrinsic mitochondrial protein) showed substantial ER contamination. Further purification of the mitochondria on a discontinuous Percoll gradient¹³ successfully eliminated ER contamination, but core protein remained associated with the mitochondria (Figure 4G).

Core Protein Effects on Cytochrome c Distribution

We next examined the effects of core protein expression on the intracellular distribution of cytochrome c. The release of cytochrome c from mitochondria can occur before or as a consequence of the mitochondrial permeability transition and may subsequently trigger the downstream events of apoptosis. We assessed the cytochrome c content of mitochondrial and cytosolic fractions prepared from Huh-7/191-20 and HeLa/191-14 cells (Figure 5A). In the presence of tetracycline (core expression off), there was minimal or no detectable cytochrome c in the cytosol. In both cell types, cytochrome c was increased in the cytosol on withdrawal of tetracycline (core expression on). Figure 5B shows the fraction of cellular cytochrome c that was recovered in the cytosolic fraction, as determined by densitometric analysis of immunoblots. The increase in cytosolic cytochrome c accompanying the expression of core was statistically significant in both Huh-7 ($P < 0.01$) and HeLa ($P < 0.05$) cells. However, most cellular cytochrome c remained in the mitochondrial fraction under these conditions.

Changes in Cellular Antioxidant Gene Expression With Induction of Core Protein

Because the relatively high levels of ROS accumulating in Huh-7/191-20 cells expressing the core protein were not associated with changes in the viability of these cells, we considered the possibility that antioxidant defense mechanisms might be induced. This hypothesis was examined by measuring the relative abun-

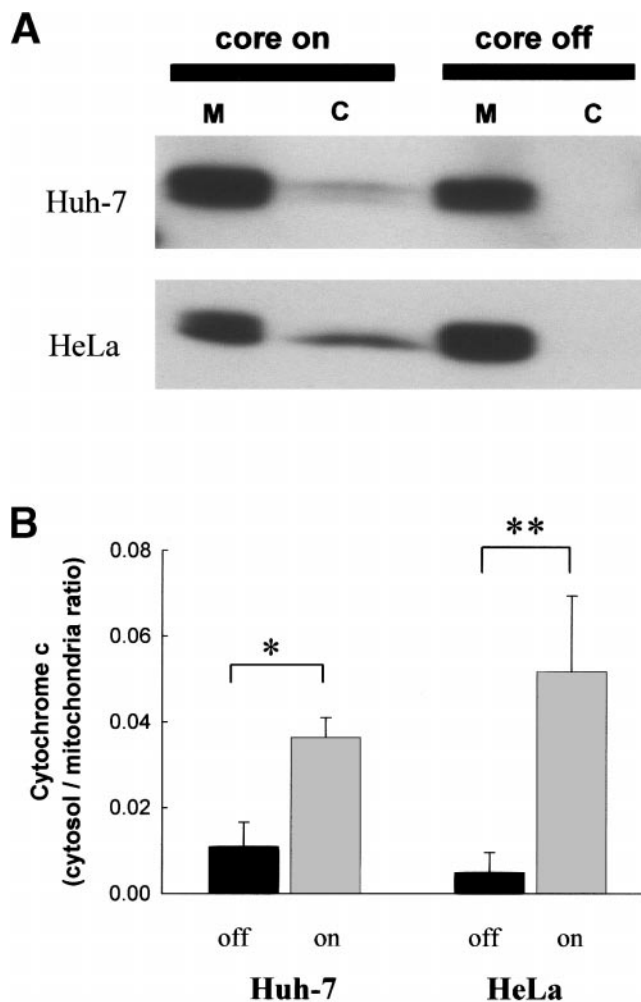


Figure 5. Distribution of cytochrome c in mitochondrial and cytosolic fractions. (A) Immunoblots for cytochrome c were performed on mitochondrial and cytosolic fractions derived from Huh-7/191-20 and HeLa/191-14 cultured in the presence or absence of tetracycline. (B) The ratio of cytochrome c concentration in cytosolic/mitochondrial fraction was measured by densitometry and corrected for the different amounts of protein applied to each lane. Results are expressed for each cell type before and after induction of core expression. * $P < 0.01$; ** $P < 0.05$.

dance of cellular RNA transcripts before and 72 hours after the induction of core protein using Affymetrix oligonucleotide microarrays containing 12,263 individual probe sets for human mRNAs. Comparison of gene expression patterns between cells expressing and not expressing HCV core showed that only 35 mRNAs were differentially regulated ≥ 3 -fold. Analysis of the identity of these gene products showed that 9 (26%) occurred in genes encoding proteins potentially involved in antioxidant defense (Table 1). The 2 mRNAs that were most increased in abundance encoded metallothionein 1A (65-fold) and metallothionein 1X (27-fold). These proteins have been shown in vitro to protect cells against oxidative damage.²⁰ The Affymetrix results were confirmed by

Table 1. Up-Regulation of Antioxidant Genes in Huh-7/191-20 Cells 72 Hours After Removal of Tetracycline

Gene name	Fold induction	GenBank ID
Metallothionein-1A	65.2	K01383
Metallothionein-1X	27.5	AA224832
Metallothionein-1F	6.8	M10943
Homo sapiens cDNA similar to MT-1F	5.4	H68340
Metallothionein-1H	5.2	R93527
Metallothionein-1E	4.7	R92331
Metallothionein-1B	4.2	M13485
Metallothionein-3	3.5	M93311
Glutathione peroxidase-like protein	3.4	X53463

independent, semiquantitative reverse-transcription polymerase chain reaction assays for these mRNAs (data not shown). Similar changes in metallothionein mRNA abundance were not observed in normal Huh-7 cells on withdrawal of tetracycline from the media.

Hepatic Lipid Peroxidation in Transgenic Mice Expressing HCV Structural Proteins

To determine the relevance of these cell culture observations to an animal model of chronic hepatitis C, we examined the response to oxidative stress in S-N/863 transgenic mice that express the HCV structural proteins (core, E1, and E2p7) under control of the liver-specific albumin promoter. These mice are immunotolerant to proteins expressed from the HCV transgene and show no evidence of intrahepatic inflammation, but male animals in the lineage have a high incidence of hepatic steatosis (Lerat et al.). To determine whether these mice are more vulnerable to oxidative injury than normal mice, we determined liver histology, hepatic lipid peroxidation, and alanine aminotransferase 24 hours after administering a low dose of CCl_4 intraperitoneally. This low dose of CCl_4 produced small foci of centrilobular necrosis with ballooning degeneration of hepatocytes and elevated alanine aminotransferase in both normal and transgenic animals. These effects are typical of CCl_4 -induced liver injury.²¹ In transgenic animals, there was a 2-fold increase in total hepatic lipid peroxidation products (Figure 6). In contrast, although nontransgenic littermates sustained a similar histologic injury, they showed no appreciable increases in hepatic lipid peroxides ($P < 0.05$). These results show that HCV transgenic animals are abnormally vulnerable to oxidant stress and that expression of the structural proteins, including the core protein, results in a tendency to develop lipid peroxidation in vivo similar to that described previously for stably transformed cell lines.

Discussion

This study used 2 different inducible cell culture systems to show that expression of the HCV core protein directly produces oxidative stress. This effect is blocked by an inhibitor of mitochondrial electron transport, and core protein itself localizes in mitochondria. Several possible mechanisms could explain a core-induced change in mitochondrial function. One explanation is that core protein alters signal transduction pathways that promote the mitochondrial permeability transition. Core protein is known to bind to the cytoplasmic domains of the lymphotoxin- β receptor²² and tumor necrosis factor receptor 1.²³ Oligomerization of each of these receptors initiates a signaling cascade that involves activation of caspase 8, proteolytic activation of Bid, and translocation of activated Bid from cytosol to mitochondria. This results in mitochondrial permeability transition, release of cytochrome c, and ultimately cellular apoptosis.²⁴

Many viruses have the ability to modulate apoptosis in their host cells, and both suppression and induction of apoptosis can be beneficial to the virus in promoting replication, persistence, and dissemination.²⁵ The mitochondrial permeability transition is a key target for viral modulation of apoptosis. Several viral proteins interact with Bcl-2 family proteins to suppress apoptosis. Examples of this are the HSV1 Us3 protein,²⁶ the HTLV-1 Tax protein,²⁷ and the HVS Bcl-2 analog protein.²⁸ Viral proteins can also activate apoptosis by multiple mechanisms. In particular, the human immunodeficiency virus 1 protein Vpr has been shown to interact directly with the mitochondrial permeability transition pore complex

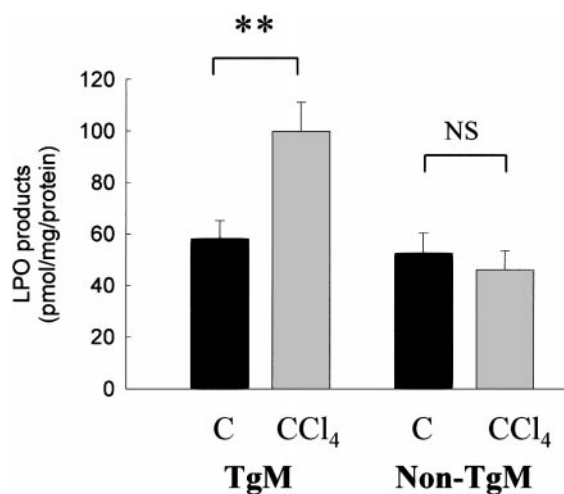


Figure 6. HCV structural protein expression sensitized oxidative stress in HCV transgenic mice. Lipid peroxide content was measured in liver homogenates 24 hours after injection of carbon tetrachloride (CCl_4) or olive oil (C) intraperitoneally to either control (non-TgM, $n = 4$) or HCV transgenic mice (TgM, $n = 5$). $**P < 0.05$.

producing cytochrome c release and apoptosis.²⁹ HCV core protein has itself been previously implicated in the modulation of apoptosis, although the reports of this phenomenon have observed both proapoptotic^{23,30,31} and antiapoptotic^{32–34} effects.

Our data suggest that direct activation of MPT is not the mechanism of the HCV core protein effects. We did not observe any increase in apoptosis in the core expressing cells, and they did not spontaneously undergo MPT. Furthermore, as shown in Figure 3B, the abnormal ROS accumulation was not blocked by treatment with cyclosporin A, an inhibitor of the mitochondrial permeability transition. Increased MPT and apoptosis is thus not the explanation for the observed increase in ROS induced by core protein. Other evidence also suggests that changes in signaling to the mitochondria are not the primary effect of core protein. In a recent study in transgenic mice, Machida et al.³² observed no change in caspase 8 or Bid activation resulting from expression of HCV proteins in the liver. In preliminary studies, we also did not observe any effect of core protein on the activation state or subcellular localization of Bid, and the treatment of cells with the nonspecific caspase inhibitor z-VADfmk did not prevent the core-associated increase in ROS (data not shown). This evidence suggests that core-induced ROS production is not a consequence of caspase-mediated signaling to the mitochondria.

An alternative hypothesis is that the core protein interacts directly with mitochondria, impairing electron transport, and thereby increasing ROS production. Core protein has been previously demonstrated to be associated with the ER³⁵ and intracellular lipid droplets.^{36,37} In our Huh-7/191-20 cells, core protein colocalized with perinuclear mitochondria, was present in purified mitochondria and ER fractions, and was expressed in structures adjacent to the mitochondria as well (Figure 4). Immunoelectron microscopy in core protein transgenic mice has also shown an association of core protein with mitochondria.³⁸ Close interactions of ER and mitochondria have also been observed in other cells and may contribute to regulation of the intramitochondrial calcium concentration.³⁹

Our evidence does not directly show a functional effect of core protein on mitochondria, but it suggests that mitochondria are the major source of the ROS because DPI, an inhibitor of electron transport in flavoenzymes, completely abolished the core-induced increment in ROS content. This inhibitor, which was not toxic to our cells under these conditions, blocks mitochondrial complex I at a proximal site and has been shown to prevent almost all mitochondrial ROS production.⁴⁰ However, DPI can

also inhibit ROS production from microsomal NADPH oxidase. Two other mitochondrial electron transport inhibitors, rotenone, a distal complex I inhibitor, and antimycin A, a complex III inhibitor, increase mitochondrial ROS production by themselves¹⁹ and thus could not provide information on the source of the core-induced ROS. Nonetheless, because mitochondria are the major source of cellular ROS and core protein directly interacts with mitochondria, these data suggest a mitochondrial source of core-induced ROS.

We observed an increase in the cytochrome c content of cytosolic fractions from core-expressing cells (Figure 4). Because the core-expressing cells did not undergo increased apoptosis or MPT, this increase in cytochrome c release could represent a change in mitochondrial fragility induced by core protein, which causes more mitochondrial disruption to occur in the isolation procedure. Our findings contrast with those of Machida et al.,³² who observed that HCV proteins inhibited Fas-mediated cytochrome c release in transgenic mice. Several important differences in the 2 experimental systems may explain these results. In the present study, cytochrome c was determined in cell cultures expressing core protein only. In the previous study,³² transgenic mice were expressing not only core protein but E1, E2, and NS2 as well. In addition, the effects observed in our study occurred without provocation, and the previous study examined cytochrome c release induced by an anti-Fas antibody.³² The magnitude of release in our study is relatively small and potentially could be overshadowed by stimuli that rapidly induce apoptosis.

Our observations suggest a new model for the pathogenesis of chronic hepatitis C, as illustrated schematically in Figure 7. An increased abundance of ROS occurs as a direct result of core protein expression. This is likely to further impair mitochondrial electron transport, amplifying the effect of core on the mitochondria and sensitizing cells to other oxidative insults. Such a posi-

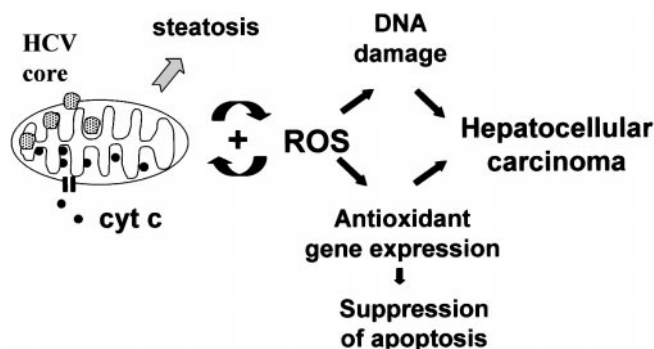


Figure 7. Model for the role of mitochondrial ROS production in pathogenesis of hepatitis C.

tive feedback effect of ROS on mitochondrial ROS generation is well documented.⁴¹ Cells use a number of antioxidant mechanisms to respond to these circumstances, including induction of antioxidant proteins that contribute to cell survival. Antioxidant gene expression could explain some of the divergent effects of core protein on apoptosis seen in other experiments.^{30,32} Different cells are likely to respond to the core-induced ROS increase in different ways. In our Huh-7/191-20 line, there is a dramatic induction of antioxidant gene expression. Core protein has been shown to activate antiapoptotic factors such as NF- κ B.⁴² This could have a net effect that suppresses apoptosis. In cells that fail to activate antioxidant genes or NF- κ B, core protein-induced ROS production may sensitize cells to apoptosis. What is consistent is that core protein expression increases cellular ROS. This interpretation is further supported by the recent report of Moriya et al.,⁴³ who have demonstrated that HCV core protein causes a state of oxidative stress in transgenic mice.

The maximal quantity of core protein expressed in our cell system is greater than that seen in liver tissue of infected humans, and it might therefore be argued that core protein plays no role in oxidative stress in human disease. However, core protein can be detected in immunoblots of infected human liver.⁴⁴ Our transgenic mice also show oxidative effects of core protein, but expression can be detected only by immunofluorescence and not by the somewhat less sensitive immunoblots (J. Sun, personal communication, June, 2001). Therefore, core protein produces oxidative stress in the range of concentrations found in infected human liver.

The consequences of this state of chronic oxidative stress include a reduction in mitochondrial metabolic processes, which might contribute to the development of steatosis by inhibition of β -oxidation and oxidative damage to both mitochondrial and chromosomal DNA. The combination of oxidative DNA damage and suppression of apoptosis favors the development of hepatocellular carcinoma. Recent observations in transforming growth factor α /c-myc mice show that chronic oxidative stress promotes hepatic tumor formation and that this can be prevented by antioxidant therapy.⁴⁵ The consequences of impaired mitochondrial function and abnormal ROS generation would be exacerbated by the immune-mediated inflammatory process present in patients with chronic hepatitis C, and the additional oxidant load it would present to the HCV-infected liver.

Given the demonstration that core protein directly induces oxidative stress, further understanding of the mechanisms of core protein's interactions with the mi-

tochondria could lead to new therapeutic approaches to this widespread chronic disease.

References

1. Davis GL. Current therapy for chronic hepatitis C. *Gastroenterology* 2000;118:S104–S114.
2. Lieber CS. Role of oxidative stress and antioxidant therapy in alcoholic and nonalcoholic liver diseases. *Adv Pharmacol* 1997; 38:601–628.
3. Barbaro G, Di Lorenzo G, Asti A, Ribersani M, Belloni G, Grisorio B, Filice G, Barbarini G. Hepatocellular mitochondrial alterations in patients with chronic hepatitis C: ultrastructural and biochemical findings. *Am J Gastroenterol* 1999;94:2198–2205.
4. Kageyama F, Kobayashi Y, Kawasaki T, Toyokuni S, Uchida K, Nakamura H. Successful interferon therapy reverses enhanced hepatic iron accumulation and lipid peroxidation in chronic hepatitis C. *Am J Gastroenterol* 2000;95:1041–1050.
5. Paradis V, Mathurin P, Kollinger M, Imbert-Bismut F, Charlotte F, Piton, Opolon P, Holstege A, Poynard T, Bedossa P. In situ detection of lipid peroxidation in chronic hepatitis C: correlation with pathological features. *J Clin Pathol* 1997;50:401–406.
6. Larrea E, Beloqui O, Muñoz-Navas MA, Civeira MP, Prieto J. Superoxide dismutase in patients with chronic hepatitis C virus infection. *Free Radic Biol Med* 1998;24:1235–1241.
7. Houghlum K, Venkataramani A, Lyche K, Chojkier M. A pilot study of the effects of d-alpha-tocopherol on hepatic stellate cell activation in chronic hepatitis C. *Gastroenterology* 1997;113:1069–1073.
8. Beard MR, Abell G, Honda M, Carroll A, Gartland M, Clarke B, Suzuki K, Lanford R, Sangar DV, Lemon SM. An infectious molecular clone of a Japanese genotype 1b hepatitis C virus. *Hepatology* 1999;30:316–324.
9. Yu H, Bauer B, Lipke GK, Phillips RL, Van Zant G. Apoptosis and hematopoiesis in murine fetal liver. *Blood* 1993;81:373–384.
10. Han Y, Weinman S, Boldogh I, Walker RK, Brasier AR. Tumor necrosis factor- α -inducible I κ B α proteolysis mediated by cytosolic m-calpain. A mechanism parallel to the ubiquitin-proteasome pathway for nuclear factor- κ B activation. *J Biol Chem* 1999;274:787–794.
11. Nieminen AL, Saylor AK, Tesfai SA, Herman B, Lemasters JJ. Contribution of the mitochondrial permeability transition to lethal injury after exposure of hepatocytes to t-butylhydroperoxide. *Biochem J* 1995;307:99–106.
12. Gross A, Yin XM, Wang K, Wei MC, Jockel J, Milliman C, Erdjument-Bromage H, Tempst P, Korsmeyer SJ. Caspase cleaved BID targets mitochondria and is required for cytochrome c release, while BCL-XL prevents this release but not tumor necrosis factor-R1/Fas death. *J Biol Chem* 1999;274:1156–1163.
13. Susin SA, Larochette N, Geuskens M, Kroemer G. Purification of mitochondria for apoptosis assays. *Methods Enzymol* 2000;322: 205–208.
14. Pierce RH, Campbell JS, Stephenson AB, Franklin CC, Chaisson M, Poot M, Kavanagh TJ, Rabinovitch PS, Fausto N. Disruption of redox homeostasis in tumor necrosis factor-induced apoptosis in a murine hepatocyte cell line. *Am J Pathol* 2000;157:221–236.
15. Honda M, Ping SH, Kaneko S, Shimazaki T, Zhang HC, Lemon SM, Kobayashi K. Hepatitis C virus core protein induces apoptosis and impairs cell cycle regulation in stably-transfected chinese hamster ovary cells. *Hepatology* 2000;31:1351–1359.
16. Fernandez-Checa JC, Garcia-Ruiz C, Colell A, Morales A, Mari M, Miranda M, Ardite E. Oxidative stress: role of mitochondria and protection by glutathione. *Biofactors* 1998;8:7–11.
17. Doussiere J, Gaillard J, Vignais PV. The heme component of the neutrophil NADPH oxidase complex is a target for arylidonium compounds. *Biochemistry* 1999;38:3694–3703.
18. Li Y, Trush MA. Diphenyleneiodonium, an NAD(P)H oxidase inhib-

- itor, also potently inhibits mitochondrial reactive oxygen species production. *Biochem Biophys Res Commun* 1998;253:295–299.
19. Bailey SM, Pietsch EC, Cunningham CC. Ethanol stimulates the production of reactive oxygen species at mitochondrial complexes I and III. *Free Radic Biol Med* 1999;27:891–900.
 20. Palmiter RD. The elusive function of metallothioneins. *Proc Natl Acad Sci U S A* 1998;95:8428–8430.
 21. Recknagel RO, Glende EA, Jr., Dolak JA, Waller RL. Mechanisms of carbon tetrachloride toxicity. *Pharmacol Ther* 1989;43:139–154.
 22. Matsumoto M, Hsieh T-Y, Zhu N, Vanarsdale T, Hwang SB, Jeng K-S, Gorbalenya AE, Lo S-Y, Ou J-H, Ware CF, Lai MMC. Hepatitis C virus core protein interacts with the cytoplasmic tail of lymphotoxin- β receptor. *J Virol* 1997;71:1301–1309.
 23. Zhu N, Khoshnan A, Schneider R, Matsumoto M, Dennert G, Ware C, Lai MMC. Hepatitis C virus core protein binds to the cytoplasmic domain of tumor necrosis factor (TNF) receptor 1 and enhances TNF-induced apoptosis. *J Virol* 1998;72:3691–3697.
 24. Kroemer G. Mitochondrial control of apoptosis: an overview. *Biochem Soc Symp* 1999;66:1–15.
 25. O'Brien V. Viruses and apoptosis. *J Gen Virol* 1998;79:1833–1845.
 26. Munger J, Roizman B. The US3 protein kinase of herpes simplex virus 1 mediates the posttranslational modification of BAD and prevents BAD-induced programmed cell death in the absence of other viral proteins. *Proc Natl Acad Sci U S A* 2001;98:10410–10415.
 27. Mori N, Fujii M, Cheng G, Ikeda S, Yamasaki Y, Yamada Y, Tomonaga M, Yamamoto N. Human T-cell leukemia virus type I tax protein induces the expression of anti-apoptotic gene Bcl-xL in human T-cells through nuclear factor-kappaB and c-AMP responsive element binding protein pathways. *Virus Genes* 2001;22:279–287.
 28. Derfuss T, Fickenscher H, Kraft MS, Henning G, Lengenfelder D, Fleckenstein B, Meinel E. Antiapoptotic activity of the herpesvirus saimiri-encoded Bcl-2 homolog: stabilization of mitochondria and inhibition of caspase-3-like activity. *J Virol* 1998;72:5897–5904.
 29. Jacotot E, Ravagnan L, Loeffler M, Ferri KF, Vieira HL, Zamzami N, Costantini P, Druillennec S, Hoebeke J, Briand JP, Irinopoulou T, Daugas E, Susin SA, Coince D, Xie ZH, Reed JC, Roques BP, Kroemer G. The HIV-1 viral protein R induces apoptosis via a direct effect on the mitochondrial permeability transition pore. *J Exp Med* 2000;191:33–46.
 30. Ruggieri A, Harada T, Matsuura Y, Miyamura T. Sensitization to Fas-mediated apoptosis by hepatitis C virus core protein. *Virology* 1997;229:68–76.
 31. Hahn CS, Cho YG, Kang BS, Lester IM, Hahn YS. The HCV core protein acts as a positive regulator of fas-mediated apoptosis in a human lymphoblastoid T cell line. *Virology* 2000;276:127–137.
 32. Machida K, Tsukiyama-Kohara K, Seike E, Tone S, Shibasaki F, Shimizu M, Takahashi H, Hayashi Y, Funata N, Taya C, Yonekawa H, Kohara M. Inhibition of cytochrome c release in Fas-mediated signaling pathway in transgenic mice induced to express hepatitis C viral proteins. *J Biol Chem* 2001;276:12140–12146.
 33. Ray RB, Meyer K, Ray R. Suppression of apoptotic cell death by hepatitis C virus core protein. *Virology* 1996;226:176–182.
 34. Marusawa H, Hijikata M, Chiba T, Shimotohno K. Hepatitis C virus core protein inhibits Fas- and tumor necrosis factor alpha-mediated apoptosis via NF- κ B activation. *J Virol* 1999;73:4713–4720.
 35. Moradpour D, Englert C, Wakita T, Wands JR. Characterization of cell lines allowing tightly regulated expression of hepatitis C virus core protein. *Virology* 1996;222:51–63.
 36. Barba G, Harper F, Harada T, Kohara M, Goulinet S, Matsuura Y, Eder G, Schaff ZS, Chapman MJ, Miyamura T, Bréchet C. Hepatitis C virus core protein shows a cytoplasmic localization and associates to cellular lipid storage droplets. *Proc Natl Acad Sci U S A* 1997;94:1200–1205.
 37. Sabile A, Perlemuter G, Bono F, Kohara K, Demaugre F, Kohara M, Matsuura Y, Miyamura T, Brechet C, Barba G. Hepatitis C virus core protein binds to apolipoprotein AII and its secretion is modulated by fibrates. *Hepatology* 1999;30:1064–1076.
 38. Moriya K, Fujie H, Shintani Y, Yotsuyanagi H, Tsutsumi T, Ishibashi K, Matsuura Y, Kimura S, Miyamura T, Koike K. The core protein of hepatitis C virus induces hepatocellular carcinoma in transgenic mice. *Nat Med* 1998;4:1065–1067.
 39. Rizzuto R, Pinton P, Carrington W, Fay FS, Fogarty KE, Lifshitz LM, Tuft RA, Pozzan T. Close contacts with the endoplasmic reticulum as determinants of mitochondrial Ca²⁺ responses. *Science* 1998;280:1763–1766.
 40. Majander A, Finel M, Wikstrom M. Diphenyleneiodonium inhibits reduction of iron-sulfur clusters in the mitochondrial NADH-ubiquinone oxidoreductase (complex I). *J Biol Chem* 1994;269:21037–21042.
 41. Cai J, Jones DP. Mitochondrial redox signaling during apoptosis. *J Bioenerg Biomembr* 1999;31:327–334.
 42. Kato N, Yoshida H, Kioko O, Kato J, Goto T, Otsuka M, Lan K, Matsushima K, Shiratori Y, Omata M. Activation of intracellular signaling by hepatitis B and C viruses: C-viral core is the most potent signal inducer. *Hepatology* 2000;32:405–412.
 43. Moriya K, Nakagawa K, Santa T, Shintani Y, Fujie H, Miyoshi H, Tsutsumi T, Miyazawa T, Ishibashi K, Horie T, Imai K, Todoroki T, Kimura S, Koike K. Oxidative stress in the absence of inflammation in a mouse model for hepatitis c virus-associated hepatocarcinogenesis. *Cancer Res* 2001;61:4365–4370.
 44. Fujie H, Yotsuyanagi H, Moriya K, Shintani Y, Tsutsumi T, Takayama T, Makuuchi M, Matsuura Y, Miyamura T, Kimura S, Koike K. Steatosis and intrahepatic hepatitis C virus in chronic hepatitis. *J Med Virol* 1999;59:141–145.
 45. Factor VM, Laskowska D, Jensen MR, Woitach JT, Popescu NC, Thorgeirsson SS. Vitamin E reduces chromosomal damage and inhibits hepatic tumor formation in a transgenic mouse model. *Proc Natl Acad Sci U S A* 2000;97:2196–2201.
-
- Received June 17, 2001. Accepted October 8, 2001.
- Address requests for reprints to: Steven A. Weinman, M.D., Department of Physiology and Biophysics, University of Texas Medical Branch, 301 University Boulevard, Galveston, Texas 77555-0641. e-mail: sweinman@utmb.edu; fax: (409) 772-3381.
- Supported in part by grants U19-AI40035 from the National Institute of Allergy and Infectious Diseases and AA12863 from the National Institute on Alcohol Abuse and Alcoholism.
- Drs. Okuda and Li authors contributed equally to this work.
- The authors thank S. Okuda for expert technical assistance, H. Fishman for assistance with confocal microscopy, S. Watowich for providing purified core protein, J. Sun for helpful discussions, and S. Ballinger and I. Boldough for their critical comments.